

## Systematic Optimization of Tokamaks for Ideal Magnetohydrodynamic Stability

L. C. Bernard and R. W. Moore

*General Atomic Company, San Diego, California 92138*

(Received 23 June 1980; revised manuscript received 22 December 1980)

High- $\beta$  plasmas, stable to all ideal magnetohydrodynamic modes, have been found by joint optimization of plasma cross sections and current profile shapes. No wall stabilization is used for the external kink. Dee cross sections are considered with varying aspect ratios. The maximum stable  $\beta$  varies from 5% at aspect ratio 4 to 10% at aspect ratio 2.5, and the optimum elongation is 1.8. The low- $n$  kink modes are the most limiting.

PACS numbers: 52.55.Gb, 52.30.+r, 52.35.Bj

Tokamak reactors become increasingly attractive for high values of  $\beta$  ( $\geq 5\%$ ), the ratio of plasma to magnetic pressure averaged over the plasma volume. Recent ideal magnetohydrodynamic (MHD) stability calculations predicted stable  $\beta$  values of 10% and above.<sup>1-3</sup> These studies assumed a superconducting wall at the plasma surface<sup>1,2</sup> or very close to it<sup>3</sup> (wall radius 20% larger than plasma radius). A superconducting wall stabilizes external kink modes, defined here as modes with small toroidal mode numbers  $0 < n \leq 3$  which perturb the plasma surface. Since the designs for future tokamaks (ETF<sup>4</sup> and INTOR<sup>5</sup>) have resistive walls, we re-examine in this paper the stability of ideal MHD modes assuming no wall stabilization of external kinks. We assume that the axisymmetric mode,  $n=0$ , can be stabilized by feedback from an appropriate poloidal coil system.

Without a wall to stabilize kink modes,  $\beta=8\%$  has been predicted for a plasma of aspect ratio 2.4, stable to all ideal MHD modes.<sup>6,7</sup> This value, higher than previous estimates,<sup>8-10</sup> was obtained by optimizing the current profile while keeping the plasma shape fixed. For an aspect ratio of 4 (typical of ETF and INTOR), similar computations predict a significantly lower  $\beta$  limit,  $\beta=3.5\%$ . We find that, by removing the fixed plasma-shape assumption and by optimizing *both* plasma shape *and* current profile, the limiting  $\beta$  is increased to 5%, similar to the design value, if the elongation is  $\sim 1.8$ .

MHD equilibria are obtained by solving the Grad-Shafranov equation:

$$R^2 \nabla \cdot (\nabla \psi / R^2) = \mu_0 R j_\varphi = -\mu_0 R^2 p' - f f', \quad (1)$$

with standard notation.<sup>2</sup> For this study we use a family of current profiles of the form

$$j_\varphi = C \{ \delta [\exp(1 - \tilde{\psi}^\alpha) - 1] R / R_c + (1 - \delta) [\exp(1 - \tilde{\psi}^\gamma) - 1] R_c / R \}. \quad (2)$$

In Eq. (2),  $\tilde{\psi} = (\psi - \psi_0) / (\psi_l - \psi_0)$ .  $\alpha$  is a measure of the width of the pressure profile;  $\alpha=1$  corresponds roughly to a typical Ohmically heated profile while larger values of  $\alpha$  give broader profiles.  $\gamma$  defines the variation of the toroidal field, and  $\delta$  varies the poloidal beta ( $\beta_p$ ). The indices 0 and  $l$  refer to the magnetic axis and limiter, respectively.  $C$  is used to normalize our equilibria to a constant toroidal current. Each equilibrium is calculated as a free-boundary problem with use of the geometry shown in Fig. 1.  $R_c$  is the geometric center of the limiter. The poloidal flux  $2\pi\psi$  is specified at the labeled points, as a model of the coils which determine the plasma shape. Up-down symmetry restricts the number of shape parameters to six. These six parameters along with  $\alpha$ ,  $\gamma$ , and  $\delta$  are optimized numerically for the maximum stable  $\beta$ . We define  $\beta = 2\mu_0 \int p dV / (B_t^2 \int dV)$  and use the definition<sup>11</sup>

$\beta_p = (\frac{1}{2}\pi) \int p dV / \int (V/V') I' d\psi$ , for which  $\beta_p=1$  when  $f'=0$ .  $B_t$  is the vacuum toroidal field measured at radius  $R_c$ . To vary the safety factor, we use the simple scaling law<sup>6</sup>

$$q_0 = c q_0, \quad f(\psi) = [f^2(\psi) + f_0^2(c^2 - 1)]^{1/2}. \quad (3)$$

To determine the stability to all ideal MHD modes, we use several distinct, complementary numerical techniques. Stability to high- $n$  modes is evaluated with the ballooning criterion in the limit of infinite toroidal mode number.<sup>12,13</sup> For computational accuracy, we also evaluate the interchange mode criterion<sup>14</sup> at the magnetic axis. Stability to low- $n$  modes is evaluated with the global code ERATO,<sup>15</sup> which computes the eigenfrequencies and eigenmodes with use of finite elements to minimize  $\delta W$ . We consider only the  $n=1$  external kink mode since, without a wall,

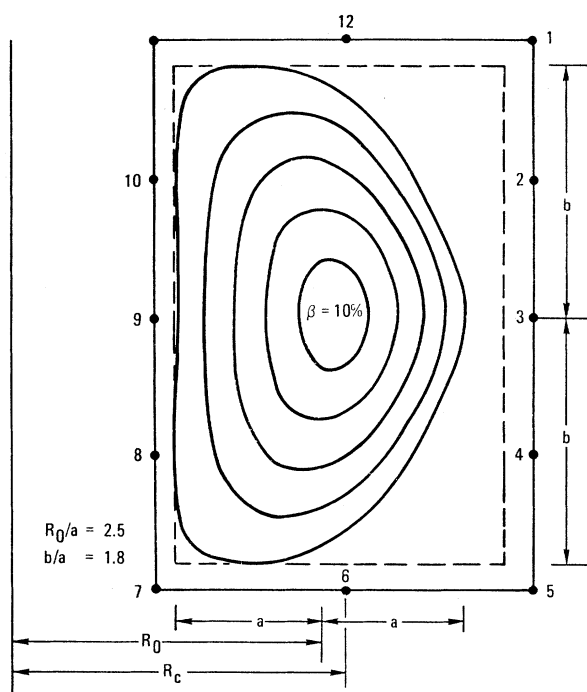


FIG. 1. Equilibrium geometry. Inner rectangle is the limiter.  $\psi$  is specified on labeled points.

this mode is more unstable than higher- $n$  kink modes.<sup>6</sup>

The optimization is automated as in Ref. 2, and takes many iterations. One iteration proceeds as follows. One of the parameters to be optimized,  $P_i$ , is incremented by  $\Delta P_i$ . An equilibrium is calculated. For that equilibrium, a critical value of  $\beta$ ,  $\beta_c$ , is calculated for marginal stability to ballooning modes by scaling the toroidal field (and  $q_0$ ). Then, if  $\beta_c$  has increased since the previous iteration, stability to the  $n=1$  external kink is evaluated, keeping  $q_0$  fixed at the critical

value for internal mode stability. If the external kink is stable, the parameters of that equilibrium are saved. The optimization is completed by sequentially varying each parameter until a maximum  $\beta_c$  is reached. Typically, 100 to 200 iterations are necessary. Computing time is reduced to 2–4 h on the Cray computer because of extensively optimized numerics and a new method used to determine stability to kink modes.

Previously,<sup>3</sup> stability has been determined by computing growth rates for a sequence of values of  $N$ , the number of mesh points, and extrapolating to  $N \rightarrow \infty$ . The numerical precision can be defined as the difference between the extrapolated zero growth rate and the smallest growth rate of the sequence. The precision on  $\lambda = |\omega^2 q_0^{-2} \omega_A^{-2}|$  has been as low as  $10^{-1}$  ( $\omega_A$  is the Alfvén frequency).<sup>3</sup> We have improved the numerics to achieve a precision of  $10^{-6}$ . With this precision, a convergence study with mesh size is not necessary, and we consider an equilibrium to be stable when the condition  $\lambda \leq 10^{-6}$  is satisfied. A better precision ( $\lambda < 10^{-6}$ ) need not be considered, as resistive effects should then be included. This new method is about ten times faster than the previous one.<sup>3</sup> At values of  $\lambda \sim 10^{-4}$ – $10^{-3}$ , ERATO finds “unstable” Alfvén continuum modes. These instabilities are purely numerical since the marginal point is the lower bound of the Alfvén continuum. These modes are localized on rational surfaces. We achieve a precision of  $10^{-6}$ , in part by accumulating  $\psi$  grid points at rational surfaces and in part by weighting points with  $dq/d\psi$ , since the shear varies greatly for high- $\beta$  equilibria. More precisely, defining  $s = \bar{\psi}^{1/2}$ ,  $\Delta s$  the distance of two adjacent points,  $N_s$  the number of radial points, and  $N_r$  the number of points accumulated near rational surfaces, the following repartition law proves adequate:

$$w(s) = \frac{1}{N_s \Delta s} = \frac{1}{3} + \frac{2}{3} \frac{N_s - N_r}{N_s} \frac{1}{q_i - q_0} q' + w_3 \sum_{k=1}^{N_k} \left[ (s - s_k)^2 + \left( \frac{N_k}{N_r(N_s - N_r)} \frac{q_i - q_0}{q_k'} \right)^2 \right]^{-1}, \quad (4)$$

where index  $k$  indicates a rational surface,  $q' = dq/ds$ , and  $w_3$  is chosen to normalize  $\int_0^1 ds w(s) = 1$ . Typically, we have chosen  $N_s = 60$ ,  $N_r = 20$ , and the number of poloidal points  $N_\chi = 40$ .

Figure 1 shows the optimum plasma shape for a plasma of aspect ratio 2.53 and elongation 1.76. The optimum  $\beta$  is 10.2% at a precision of  $10^{-6}$  for kink mode stability and only changes to 10.4% at a precision of  $10^{-4}$ . The shape is triangular at the outside edge of the plasma and straight on the inside edge. Triangularity at the outside edge

minimizes the plasma volume in the region unfavorable to the kink. It also decreases the connection length between bad and good curvature regions which improves ballooning mode stability. In contrast to Ref. 2, there is no indentation at the inside edge (favorable to the ballooning mode) in order to minimize the amount of current flowing close to the surface.

The optimum current profile is broad and  $\beta_p < 1$ , giving a safety factor at the surface  $q_i \sim 3$ .

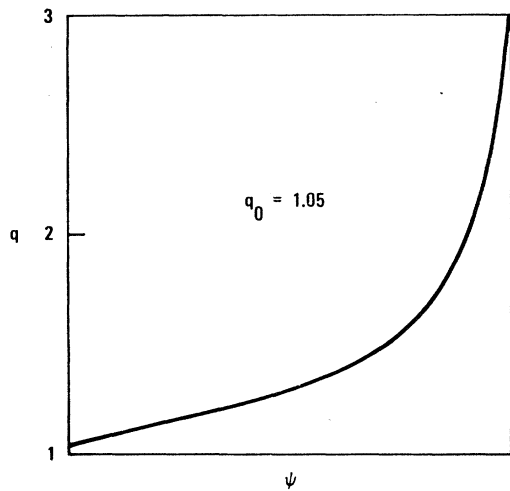


FIG. 2. Safety-factor profile for the equilibrium shown in Fig. 1.

This low value of  $\beta_p$  yields flux surfaces well centered inside the plasma surface and reduces the current gradient at the outside edge, a good effect for stability to the external kink. For the optimum shape and current profile ( $\beta_p < 1$ ), the marginal stability value of  $q_0$  for ballooning modes is less than one. In contrast, the internal kink limits  $q_0 > 1$ . The external kink is then the mode which limits  $\beta$ . The optimum  $q$  profile (Fig. 2) shows small shear inside the plasma and strong shear close to the plasma surface. The pressure profile is bell shaped, as expected.

We have repeated the same computations for different aspect ratios, keeping the elongation of the limiter box fixed and equal to 1.5. Figure 3

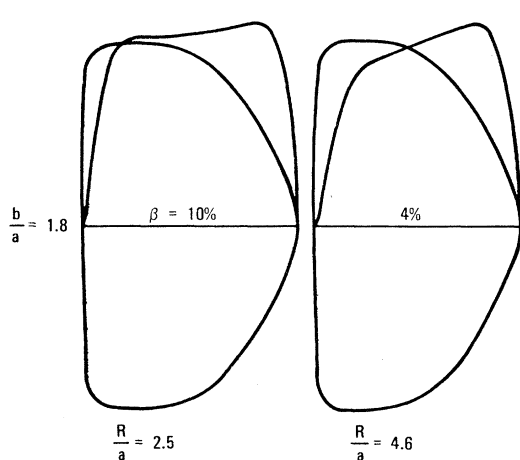


FIG. 3. Examples of optimum shapes and current profiles at different aspect ratios.

TABLE I. Optimum  $\beta_c$ ,  $\beta_p$ , and current profile parameters for different aspect ratios. For comparison, we include the definition (Refs. 8 and 10)  $\beta^* = 2\mu_0(\int p^2 dV \int dV)^{1/2} / (B_i^2 \int dV)$ .

$R_0/a$	$b/a$	$\beta$ (%)	$\beta^*$ (%)	$\beta_p$	$\alpha$	$\gamma$	$\delta$
2.53	1.76	10.2	13.1	0.53	5.5	5.5	0.6
3.18	1.90	7.16	9.49	0.64	4	7.34	0.741
3.86	1.89	5.10	6.78	0.78	4.2	5.15	0.826
4.59	1.82	3.8	5.09	0.99	4	6.85	0.995

shows examples of optimum shape and current profiles, and Table I shows optimum values of  $\beta$  and  $\beta_p$ . Since the plasma shape is optimized, the elongation values shown in Table I represent optimum values. This is verified by repeating our computations with a limiter elongation equal to 2, and obtaining similar results. The data of Table I may be fitted approximately with a scaling law  $\beta \propto (R_0/a)^{-3/2}$ . By interpolating the values of Table I, we find  $\beta = 5\%$  at aspect ratio 4 and elongation 1.8. This is comparable to the recommended design value of ETF<sup>4</sup> and INTOR.<sup>5</sup> Higher values of  $\beta$  could be obtained by reducing the aspect ratio or by using a wall to stabilize external kinks.

In summary, the results of our combined optimization of plasma and current shaping are as follows: (i) optimum plasma shape and current profiles are similar for different aspect ratios; (ii) the optimum plasma shape is triangular at the outside edge and straight on the inside edge; (iii) the optimum current profile is broad and  $\beta_p$  is less than unity; (iv) the optimum elongation is approximately 1.8; (v) provided internal kink mode stability is attained by forcing  $q$  on axis to be above unity, we find that the most restrictive modes are the low- $n$  external modes and not the high- $n$  ballooning modes.

We thank R. L. Miller, G. E. Guest, F. J. Helton, D. Dobrott, W. Kerner, and R. Gruber for stimulating discussions, and B. Davidson and B. Dy for programming assistance. This work was supported by the U. S. Department of Energy, Contract No. DE-AT03-76ET51011.

<sup>1</sup>A. Sykes, J. A. Wesson, and S. J. Cox, Phys. Rev. Lett. **39**, 757 (1977).

<sup>2</sup>R. L. Miller and R. W. Moore, Phys. Rev. Lett. **43**, 765 (1979).

<sup>3</sup>L. A. Charlton *et al.*, Phys. Rev. Lett. **43**, 1395

(1979).

<sup>4</sup>Y.-K. M. Peng *et al.*, Bull. Am. Phys. Soc. **24**, 947 (1979) [Engineering Test Facility (ETF)].<sup>5</sup>P. H. Rutherford, Bull. Am. Phys. Soc. **24**, 1010 (1979) [International Tokamak Reactor (INTOR)].<sup>6</sup>L. C. Bernard *et al.*, Nucl. Fusion **20**, 1199 (1980).<sup>7</sup>W. Kerner *et al.*, in *Proceedings of the Ninth European Conference on Controlled Fusion and Plasma Physics, Oxford, England, 1979*, edited by R. J. Bickerton (Culham Laboratory, Oxford, England, 1979), Vol. I, p. 9.<sup>8</sup>A. M. M. Todd *et al.*, Phys. Rev. Lett. **38**, 826 (1977).<sup>9</sup>D. Berger, Ph.D. thesis, Lausanne, 1977 (unpublished).<sup>10</sup>A. M. M. Todd *et al.*, Nucl. Fusion **19**, 743 (1979).<sup>11</sup>L. E. Zakharov and V. D. Shafranov, Zh. Tech. Fiz. **43**, 225 (1973) [Sov. Phys. Tech. Phys. **18**, 151 (1973)].<sup>12</sup>D. R. Dobrott *et al.*, Phys. Rev. Lett. **39**, 943 (1977).<sup>13</sup>J. W. Connor *et al.*, Phys. Rev. Lett. **40**, 396 (1978).<sup>14</sup>C. Mercier, Nucl. Fusion **1**, 47 (1970).<sup>15</sup>R. Gruber *et al.*, to be published.

## Heat-Capacity Study of the Transition from a Stacked-Hexatic-*B* Phase to a Smectic-*A* Phase

C. C. Huang and J. M. Viner

*School of Physics and Astronomy, University of Minnesota, Minneapolis, Minnesota 55455*

and

R. Pindak and J. W. Goodby

*Bell Laboratories, Murray Hill, New Jersey 07974*

(Received 26 February 1981)

High-resolution ac calorimetry measurements have been performed on a liquid-crystal material exhibiting a stacked-hexatic-*B*-smectic-*A* phase transition. The transition appears to be second order with a pronounced, symmetric heat capacity peak and no observable thermal hysteresis. The data can be fitted by a power law divergence with critical exponents  $\alpha = \alpha' = 0.64 \pm 0.04$  and a ratio of critical amplitudes  $A/A' = 0.83$ . Measurements have also been carried out on a crystalline-*B*-smectic-*A* transition which is found to be first order.

PACS numbers: 64.70.Ew, 61.30.-v

It is well known that some liquid-crystal materials exhibit a layered phase with hexagonal in-plane ordering.<sup>1</sup> This phase is referred to as a smectic *B* or, simply, *B* phase. Recent experiments<sup>2-8</sup> have established that, among the *B* phases in different materials, there are two microscopically distinct types. The first type is a crystalline phase. X-ray measurements<sup>2</sup> demonstrated that this *B* phase has long-range, three-dimensional (3D) positional order. Its crystalline nature was confirmed by mechanical measurements which showed that this phase supports a shear both within<sup>3,4</sup> and between<sup>5</sup> its layers. The second type of *B* phase was first identified by its lack of interlayer correlations.<sup>6</sup> A detailed x-ray study<sup>7</sup> demonstrated that the second *B* phase has only short-range in-plane positional order but long-range 3D sixfold bond-orientational order. The mechanical measurements<sup>8</sup> demonstrated that the second *B* phase does not support an in-plane shear.

The possibility of a phase characterized by bond-orientational order was first discussed in the context of two-dimensional (2D) melting.<sup>9,10</sup> A bond-orientationally ordered phase (a hexatic phase)

was predicted to occur between the 2D solid and liquid if 2D melting was a dislocation-mediated second-order phase transition. Subsequently, a 3D liquid-crystal phase was proposed which consisted of stacked, interacting 2D hexatic layers.<sup>11</sup> The structural and mechanical properties of the second *B* phase are those expected for this 3D stacked hexatic phase. We, therefore, refer to the first type of *B* phase as a crystalline *B* and the second as a hexatic *B*. Both *B* phases can melt into a higher temperature smectic-*A* (*A*) phase with fluidlike layers.

In this paper we report detailed heat-capacity measurements on the hexatic-*B*-*A* transition. This transition is important to study because the liquid-crystal hexatic *B* phase is the only system in which the existence of hexatic ordering has been proven. We will also report measurements on the crystalline-*B*-*A* transition which we find to be first order. In contrast, the hexatic-*B*-*A* transition is second order exhibiting a symmetric heat-capacity peak with no observable thermal hysteresis.

The liquid-crystal compounds that we chose to study were *N*-(4-*n*-butyloxybenzylidene)-4-*n*-